Inorganic Chemistry

Communication

pubs.acs.org/IC

Tracing the Sources of the Different Magnetic Behavior in the Two Phases of the Bistable $(BDTA)_2[Co(mnt)_2]$ Compound

Sergi Vela, Mercè Deumal,* Jordi Ribas-Arino,* and Juan J. Novoa

Departament de Química Física & IQTCUB, Facultat de Química, Universitat de Barcelona, Martí i Franquès 1, Barcelona, Spain

Supporting Information

ABSTRACT: A complete computational study of the magnetic properties of the two known phases of the bistable $(BDTA)_2[Co(mnt)_2]$ compound is presented. The origin of their different magnetic properties can be traced to a variation in the values of the **g** tensor, together with a hitherto unknown change in the J_{AB} values and their magnetic topology.

In the quest for new technologies suitable for future memory and switching devices, molecular materials that can be switched between two states by the application of an external stimulus (e.g., heat, pressure) have attracted much attention.[1−3] For these bistable materials to be of technological interest, the phase transitions between the two polymorphs must be abrupt, besides presenting a hysteresis loop.[3,4] Despite the plethora of materials exhibiting these properties,[5−8] a rational design of new molecule-based bistable materials is not yet fully attainable because there is no proper knowledge of the mechanism responsible for this behavior at the microscopic level.[9]

$(BDTA)_2[Co(mnt)_2]$ (**1**) is a remarkable bistable system reported by Awaga and co-workers,[10,11] whose two polymorphic phases present different magnetic properties (BDTA = 1,3,2-benzodithiazolyl; mnt^{2-} = maleonitriledithiolate). Each neutral $(BDTA)_2[Co(mnt)_2]$ unit presents a doublet ground state [the geometries, singly occupied molecular orbitals (SOMOs), and spin densities for both phases can be found in the Supporting Information]. The different magnetic properties of the two phases of **1** were originally explained solely in terms of a change in the **g**-tensor value upon phase transition. This is in contrast with other bistable systems, where variation in the magnetic properties was traced to changes in the values of the microscopic exchange interactions, J_{AB}, on going from one phase to another one.[12] Such a different interpretation prompted us to carry out a theoretical first-principles bottom-up (FPBU)[13] study where the shape of the magnetic susceptibility curves of the two phases of **1** was investigated over the whole range of experimentally measured temperatures (0−300 K). On the basis of this study, we have been able to provide a sound explanation for the different magnetic properties of the two phases of **1**.

As observed in Figure 1a, **1** exhibits an abrupt jump in the experimental χT (χ = molar magnetic susceptibility) at ca. 190 K with a hysteresis width of 20 K.[10] Such a transition, in addition to changes in the crystal symmetry and packing, is accompanied by the formation/cleavage of an axially coordinated Co···S bond, involving one sulfur atom of

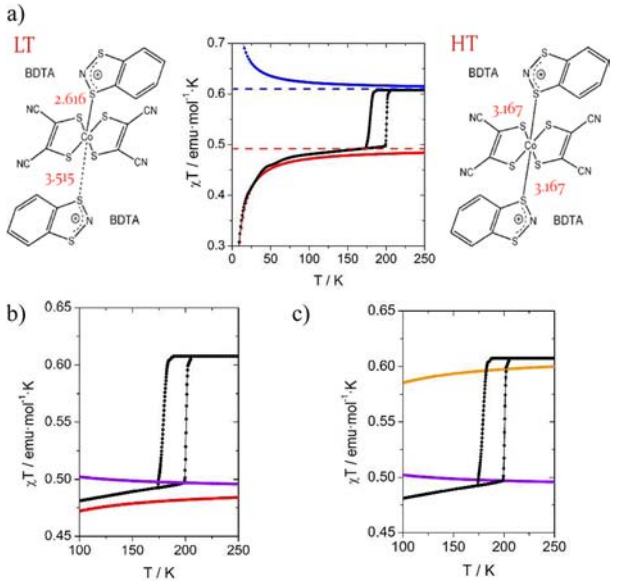

Figure 1. Comparison between the experimental (black) and computed χ curves: (a) using the computed J_{AB} values and the experimental **g** tensors for each phase (HT−g^{HT} and LT−g^{LT} curves are in blue and red, respectively; dashed lines correspond to χT values obtained for both phases when all J_{AB} interactions are set to zero, corresponding to the Curie law regime); (b) keeping the computed J_{AB} values but forcing the **g** tensor for both phases to be equal to that for LT (HT−g^{LT} and LT−g^{LT} curves in purple and red, respectively); (c) keeping the **g** tensor but exchanging magnetic topology between the HT and LT phases (HT−g^{LT} and LT−g^{HT} in purple and orange, respectively). The geometries of the $(BDTA)_2[Co(mnt)_2]$ units in the LT and HT phases are displayed in part a.

BDTA. The origin of such a jump in χT has been previously attributed[10] to a change in the **g** tensor of **1** [from 2.55 at high temperature (HT) to 2.29 at low temperature (LT)] due to a charge-transfer process that takes place when this Co···S bond is formed/broken.[10] Theoretical calculations have confirmed such metal-to-ligand charge transfer.[14] Although it is well-known[12,15] that the size of the magnetic exchange J_{AB} interactions and their magnetic topology (the network of connectivity that the non-negligible J_{AB} interactions build within the crystal) are essential in defining the macroscopic magnetic properties, the changes in the J_{AB} values and their topology upon phase transition surprisingly have not yet been

Received: May 24, 2012
Published: July 31, 2012

   dx.doi.org/10.1021/ic301085t | *Inorg. Chem.* 2012, 51, 8646−8648

addressed. The reason might be 2-fold: (i) a lack of good models to fit the experimental $\chi T(T)$ data for bulk magnetic systems and (ii) the shape of the χT curve in the HT phase, which hints at the existence of very small J_{AB} values. One should thus wonder about the impact of the J_{AB} values and their topology on the χT curves for the HT and LT polymorphs of **1** and, particularly, on the shape of the hysteresis cycle.

The J_{AB} interactions for all unique radical pairs present in the HT and LT crystal structures of **1** and, based on them, the χT curves have been evaluated using our FPBU work strategy.[13] For the LT polymorph characterized at 100 K, five unique **1**···**1** radical pairs were found to present a nonnegligible[16] J_{AB} value (their Co···Co distances ranging from 6.72 to 9.31 Å; see Table 1 and the Supporting Information). Analogously, two non-

Table 1. Magnetic Exchange Coupling J_{AB} (in cm^{-1}) for LT and HT Phases of 1 Computed with (i) a Basis Set of TZV Quality and (ii) a def2-tzvp Basis Set (in Parentheses)[a]

LT		HT	
d(Co···Co)	J_{AB}	d(Co···Co)	J_{AB}
6.792	−3.3 (−3.6)	7.017	0.3 (0.3)
7.212	−0.5	7.275	1.5 (1.9)
8.605	−0.2		
8.391	−2.4		
9.313	0.2		

[a]Also given are the corresponding Co···Co distances (in Å).

negligible **1**···**1** radical pairs were found in the HT polymorph characterized at 253 K. Using these J_{AB} values and the magnetic topologies that they define (see below), one can compute the χT curves with the experimental values[10] for the **g** tensor: g^{LT} = 2.29 for LT and g^{HT} = 2.55 for HT (Figure 1a).[17] Note that the computed χT curves properly reproduce not only the experimental curves for the LT and HT polymorphs *over the whole range of temperatures* but also the gap between them. Also note that while the χT^{LT} curve is dominated by antiferromagnetic (AFM) interactions, the χT^{HT} curve is dominated by ferromagnetic (FM) interactions, consistent with the results collected in Table 1. Such an important change in the sign of the magnetic interaction can be attributed not only to geometrical changes but also to noticeable differences in the topology of the spin density of the $(BDTA)_2[Co(mnt)_2]$ units in both phases (see Figure 2 and the Supporting Information).

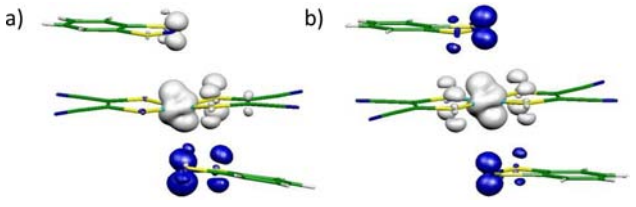

Figure 2. Spin densities of complex **1** for the (a) LT and (b) HT phases.

There is no experimental data to confirm the dominant FM nature of the HT phase at low temperature. Calculations with the larger def2-tzvp[18] basis set on selected dimers of the HT and LT phases confirm the accuracy of the computed J_{AB} values and their topologies (see the Supporting Information). Previous experience on other FM systems indicates that the FPBU methodology provides an appropriate description of the J_{AB} microscopic parameters and macroscopic properties in the region of temperatures for HT/LT phase transition.[15]

One can now analyze the relative importance of the **g** tensor on the $\chi T^{HT}-\chi T^{LT}$ jump present in **1** (Figure 1). This can be evaluated by comparing the previously computed $\chi T^{HT}-g^{HT}$ and $\chi T^{LT}-g^{LT}$ curves (Figure 1a) with those obtained using the same **g** tensor (e.g., g^{LT}=2.29) for both phases (see Figure 1b). A comparison of the χT^{HT} curves in parts a (blue) and b (purple) of Figure 1 shows that the latter curve is significantly shifted downward in the whole temperature range. The $[\chi T^{HT}-g^{LT}]-[\chi T^{LT}-g^{LT}]$ jump in Figure 1b at ca. 190 K, whose origin is exclusively due to J_{AB} interactions, is around a nonnegligible 16% of the experimental jump at the same temperature. Besides, Figure 1c clearly shows that the magnetic topology plays a key role in tuning the slope of the χT curves within the hysteresis loop; i.e., if one uses the wrong magnetic topology with the correct g factor in the LT ($\chi T^{HT}-g^{LT}$) phase (and vice versa), the slope of the resulting χT curve has the opposite sign compared to experiment. All of these results prove that changes in both the g factor and magnetic topology are indeed at the origin of the hysteresis behavior.

The different magnetic susceptibilities of the HT and LT phases can be better understood by inspecting in detail their magnetic topologies (see Figure 3 and the Supporting

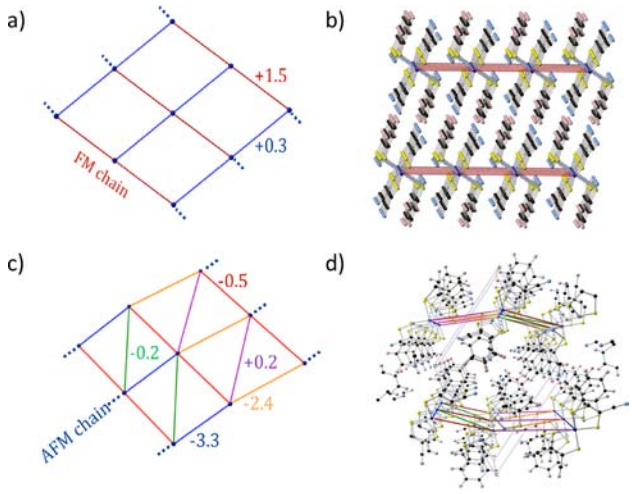

Figure 3. Magnetic topologies for the (a and b) HT and (c and d) LT phases. The colored lines represent J_{AB} (in cm^{-1}) between radicals (blue dots). (a and c) Isolated 2D magnetic layers. (b and d) Views of the magnetic topologies within the crystal packing consisting of magnetically isolated 2D planes.

Information). Each phase can be visualized as the repetition of a magnetic building block along the symmetry elements of the crystal. The magnetic building block for the HT phase has rhomboidal shape, with FM exchange couplings in the long and short edges (Table 1). This pattern gives rise to 2D planes, consisting of a set of weakly interacting (+0.3 cm^{-1}) FM chains (+1.5 cm^{-1}) (Figure 3a). These 2D planes stack in the third dimension, although remaining magnetically isolated (Figure 3b). The rhomboidal shape of the magnetic building block observed in HT is basically preserved in the LT phase (Table 1) but with relevant modifications. First of all, the 2D planes in LT are corrugated and can now be seen as a set of alternating 1D AFM chains (−3.3 and −2.4 cm^{-1}) that weakly interact among them (Figure 3c). The planes stack along the third direction, and the resulting overall magnetic topology is, once

dx.doi.org/10.1021/ic301085t | Inorg. Chem. 2012, 51, 8646−8648

again, a pile of magnetically isolated 2D planes (Figure 3d). Therefore, analysis of these two magnetic topologies clearly explains why the χT^{LT} curve is dominated by AFM interactions, whereas χT^{HT} presents dominant FM interactions (see Figure 1), and this allows one to associate these dominant interactions with specific radical pairs.

In summary, by doing a FPBU study[13] of the magnetic interactions in the LT and HT phases of **1**, we have gained a full understanding of the changes in the magnetic properties upon phase transition of the bistable compound **1**. Using the computed J_{AB} values and their topologies, we have reproduced and rationalized the experimental χT curves in the whole range of measured temperatures, including the hysteresis loop present in the bistability region. Our calculations allow us to trace the origin of the jump in the HT and LT χT curves mainly to variation in the **g** tensor, in good agreement with previous approximations.[10] Yet, the role of the J_{AB} interactions must not be neglected. In fact, the dominant AFM behavior of the experimental χT^{LT} curve at low temperatures can only be reproduced once the J_{AB} values are also taken into consideration. For the χT^{HT} curve, our study uncovers a dominant FM behavior. This LT change from a dominant FM (HT phase) to a dominant AFM (LT phase) behavior suggests the possibility of new photomagnetic studies. Overall, this work constitutes another example of how theoretical calculations can provide a most valuable insight to interpret, rationalize, and predict the magnetic properties of molecule-based materials.

Computational Details. On the basis of the FPBU work strategy,[13] all symmetry-unique radical···radical **1**···**1** exchange couplings (J_{AB}) were calculated for dimers extracted from the crystal structure (selected by considering a cutoff distance of 10 Å between cobalt atoms; see the Supporting Information for the dimer geometries). The radicals here are doublets ($S = {}^1/_2$). For the Heisenberg Hamiltonian $\hat{H} = -2\sum_{A,B}^{N} J_{AB}\hat{S}_A \cdot \hat{S}_B$, the value of J_{AB} for each AB pair is computed as the energy difference between the pair open-shell singlet S and triplet T states, $\Delta E^{S-T} = 2(E^{BS} - E^{T}) = 2J_{AB}$ (note that the broken symmetry, BS, approach[19] was used to properly describe the open-shell singlet state). Energy evaluations were first done using the B3LYP[20] functional, as implemented in *Gaussian03*,[21] with the TZV basis set[22] for cobalt atoms and the 6-31+G* basis set[23] for the remaining atoms. The **g**-tensor calculations were done with *ORCA2.7*[24] (see Supporting Information).

■ ASSOCIATED CONTENT

Ⓢ Supporting Information

Details on the electronic structures of radical **1**, assessment of the accuracy of the J_{AB} calculation, and selected magnetic models for χT simulation. This material is available free of charge via the Internet at http://pubs.acs.org.

■ AUTHOR INFORMATION

Corresponding Author

*E-mail: j.ribas@ub.edu (J.R.-A.), merce.deumal@ub.edu (M.D.).

Notes

The authors declare no competing financial interest.

■ ACKNOWLEDGMENTS

We are thankful for support of the Spanish Government (Projects MAT2008-02032 and MAT2011-25972), a Ph.D. grant to S.V., and a "Ramón y Cajal" fellowship to J.R.-A. We are also thankful to the Catalan DURSI (Grant 2009-SGR-1203) and for computer time allocated by CESCA and BSC.

■ REFERENCES

(1) Balzani, V.; Credi, A.; Venturi, M. *Molecular Devices and Machines. A Journey into the Nanoworld*; Wiley-VCH: New York, 2003.
(2) Kahn, O.; Martínez, C. J. *Science* **1998**, *279*, 44.
(3) Létard, J.-F.; Guionneau, P.; Goux-Capes, L. *Top. Curr. Chem.* **2004**, *235*, 221.
(4) Kahn, O.; Launay, J. P. *Chemtronics* **1988**, *3*, 140.
(5) Sato, O.; Tao, J.; Zhang, Y.-Z. *Angew. Chem., Int. Ed.* **2007**, *46*, 2152.
(6) Transition-metal spin-crossover complexes: (a) Gütlich, P.; Goodwin, H. A. *Top. Curr. Chem.* **2004**, *233*, 1. (b) Gamez, P.; Costa, J. S.; Quesada, M.; Aromí, G. *Dalton Trans.* **2009**, 7845. (c) Halcrow, M. A. *Chem. Soc. Rev.* **2011**, *40*, 4119.
(7) Purely organic radical compounds: (a) Fujita, W.; Awaga, K. *Science* **1999**, *286*, 261. (b) Itkis, M. E.; Chi, X.; Cordes, A. W.; Haddon, R. C. *Science* **2002**, *296*, 1443. (c) Hicks, R. G. *Nat. Chem.* **2011**, *3*, 189.
(8) Charge-transfer complexes: (a) Hendrickson, D. N.; Pierpoint, C. G. *Top. Curr. Chem.* **2004**, *234*, 63. (b) Berlinguette, C. P.; Dragulescu-Andrasi, A.; Sieber, A.; Galan-Mascaros, J. R.; Güdel, H.-U.; Achim, C.; Dunbar, K. R. *J. Am. Chem. Soc.* **2004**, *126*, 6222. (c) Sessoli, R. *Nat. Chem.* **2010**, *2*, 346.
(9) Real, J. A.; Gaspar, A. B.; Niel, V.; Muñoz, M. C. *Coord. Chem. Rev.* **2003**, *236*, 121.
(10) Umezono, Y.; Fujita, W.; Awaga, K. *J. Am. Chem. Soc.* **2006**, *128*, 1084.
(11) Fujita, W.; Awaga, K.; Nakazawa, Y.; Saito, K.; Sorai, M. *Chem. Phys. Lett.* **2002**, *352*, 348.
(12) For instance, see: (a) Clarke, C. S.; Jornet-Somoza, J.; Mota, F.; Novoa, J. J.; Deumal, M. *J. Am. Chem. Soc.* **2010**, *132*, 17817. (b) Rawson, J. M.; Alberola, A.; Whalley, A. *J. Mater. Chem.* **2006**, *16*, 2560. (c) Lekin, K.; Winter, S. M.; Downey, L. E.; Bao, X.; Tse, J. S.; Desgreniers, S.; Secco, R. A.; Dube, P. A.; Oakley, R. T. *J. Am. Chem. Soc.* **2010**, *132*, 16212.
(13) Deumal, M.; Bearpark, M. J.; Novoa, J. J.; Robb, M. A. *J. Phys. Chem. A* **2002**, *106*, 1299.
(14) Kepenekian, M.; Le Guennic, B.; Awaga, K.; Robert, V. *Phys. Chem. Chem. Phys.* **2009**, *11*, 6066.
(15) (a) Novoa, J. J.; Deumal, M.; Jornet-Somoza, J. *Chem. Soc. Rev.* **2011**, *40*, 3182. (b) Norel, L.; Rota, J.-B.; Chamoreau, L.-M.; Pilet, G.; Robert, V.; Train, C. *Angew. Chem.* **2011**, *123*, 7266. (c) Vérot, M.; Bréfuel, N.; Pécaut, J.; Train, C.; Robert, V. *Chem.—Asian J.* **2012**, *7*, 380.
(16) J_{AB} values whose absolute value is larger than 0.05 cm^{-1}.
(17) Our computed **g** tensor values on a $(BDTA)_2[Co(mnt)_2]$ moiety are $g^{LT} = 2.18$ and $g^{HT} = 2.22$ to be compared to experimental $g^{LT} = 2.29 \pm 0.10$ and $g^{HT} = 2.55 \pm 0.10$ data.[10] Thus, we have opted for the combined use of experimental data together with computed J_{AB} values, which has already been proven to be a successful strategy. See ref 15a and Petit, S.; Borshch, S. A.; Robert, V. *J. Am. Chem. Soc.* **2003**, *125*, 3959.
(18) Weigend, F.; Ahlrichs, R. *Phys. Chem. Chem. Phys.* **2005**, *7*, 3297.
(19) (a) Noodleman, L. *J. Chem. Phys.* **1981**, *74*, 5737. (b) Noodleman, L.; Davidson, E. R. *Chem. Phys.* **1986**, *109*, 131.
(20) Becke, A. D. *J. Chem. Phys.* **1996**, *104*, 1040.
(21) Frisch, M. J. et al. *Gaussian 03*, revision C.02; Gaussian, Inc.: Wallingford, CT, 2004.
(22) Schaefer, A.; Huber, C.; Ahlrichs, R. *J. Chem. Phys.* **1994**, *100*, 5829.
(23) Ditchfield, R.; Hehre, W. J.; Pople, J. A. *J. Chem. Phys.* **1971**, *54*, 724.
(24) Neese, F. *WIREs Comput. Mol. Sci.* **2012**, *2*, 73.